Automatic segmentation of thigh magnetic resonance images

Lorena Urricelqui, Armando Malanda., and Arantxa Villanueva

Abstract— **Purpose:** To develop a method for automatic segmentation of adipose and muscular tissue in thighs from magnetic resonance images.

Materials and methods: Thirty obese women were scanned on a Siemens Impact Expert 1T resonance machine. 1500 images were finally used in the tests. The developed segmentation method is a recursive and multilevel process that makes use of several concepts such as shaped histograms, adaptative thresholding and connectivity. The segmentation process was implemented in Matlab and operates without the need of any user interaction. The whole set of images were segmented with the developed method. An expert radiologist segmented the same set of images following a manual procedure with the aid of the SliceOmatic software (Tomovision). These constituted our 'goal standard'.

Results: The number of coincidental pixels of the automatic and manual segmentation procedures was measured. The average results were above 90 % of success in most of the images.

Conclusions: The proposed approach allows effective automatic segmentation of MRIs from thighs, comparable to expert manual performance.

Keywords—segmentation, thigh, magnetic resonance image, fat, muscle

I. Introduction

OBESITY is considered to be a factor of risk in diverse chronic pathologies in the developed world, such as Type n diabetes, hypertension, arteriosclerosis, cardiovascular diseases, etc. Magnetic resonance images (MRI) may be used to measure the volumes of fat and muscle from these patients in order to evaluate therapies to reduce fat and increase muscular mass. The high spatial resolution and harmless behaviour that offers MRI compared to other technologies based on ionizing radiation are determinant in its daily use. It is therefore of interest to develop techniques to identify and quantify these tissues from the images.

A number of software packages and methodologies that segment thigh images can be found [1]. They exhibit varied complexity and degree of automation. Manual and semi-automated segmentation [2-5] are not very helpful in dealing with large amounts of images. So, from the user's point of view, one of the objectives is to find a segmentation method that needs the minor degree of intervention. In this respect, two almost automatic tools have been recently proposed by Positano et al. [6-7] and by Liou et al. [8], which are based on active contours and adapted threshold algorithms, respectively. However, these approaches seem to suffer some limitations due to the lack of contrast in the border of the tissues. The progressive variation of the intensity levels in the image induces segmentation errors, making it necessary the intervention of an expert to ensure a correct segmentation.

The objective of the work presented here is to develop a reliable automatic tool of segmentation of MRI, in order to separate and to determine the volume and distribution of adipose and muscular tissue of the thigh. The results are compared to images manually marked by an expert radiologist with the aid of the SliceOmatic (Tomovision Inc.) image processing tool.

II. Material and methods

A. Materials

The study was carried out with thigh images of 30 obese women of medium age (34-47) using a Siemens Impact Expert 1T resonance machine. From each subject, 30 slices were taken from the hip down to the knee with a 1 cm separation. Each one undertook the experiment twice. In each acquisition, 30 slices were taken, form hip to knee, the last 5 of this were discarded due to the presence of tendons and the reduced gray level contrast of muscle and fat tissue.

The Matlab (Mathworks Inc) programming environment, including the Image Processing Toolbox was used to develop the programs for this study. As already mentioned, SliceOmatic (Tomovision Inc.) image processing tool was also employed to help the expert in the manual marking of the images.

B. Methods

Fat tissue usually presents higher intensity level than muscle tissue in thigh MRIs, while background is supposed to be darker, almo st black. Thus, intensity thresholding seems the

Lorena Urricelqui is with the Electrical and Electronics Engineering Department, Universidad Publica de Navarra. Campus Arrosadia,. 31006 Pamplona (SPAIN)

Armando Malanda is with the Electrical and Electronics Engineering Department, Universidad Publica de Navarra. Campus Arrosadia,. 31006 Pamplona (SPAIN) (e-mail: malanda@unavarra.es)

Arantxa Villanueva is with the Electrical and Electronics Engineering Department, Universidad Publica de Navarra. Campus Arrosadia,. 31006 Pamplona (SPAIN)

World Academy of Science, Engineering and Technology
International Journal of Biomedical and Biological Engineering
Vol:3, No:10, 2009

most reasonable approach to perform this segmentation. However, the intensity source in resonance images is not uniform and the pixels corresponding to the same tissue suffer significant variations of intensity.

The main technique used in our approach is adapted thresholding [9], where the image is divided in smaller subimages and basic thresholding is applied independently to each subimage. Finally the results of the different segmentations have to be joined in an overall segmentation. Bones are also present in thigh images occupying central position in the limbs, surrounded by muscles. Bone tissue has usually lighter intensity levels than muscle tissue, and comparable to that of fat. So a particular procedure has to be included to isolate the image region corresponding to the bone. The overall method is implemented in four stages, explained thereafter:

1) Image division and segmentation of subimages
2) Creation of templates
3) Bone extraction
4) Final segmentation

1) Image division and segmentation of subimages

This stage is an iterative and recursive process that comprises four iterations or levels of depth where the following actions are carried out:

- Division of the image
- Histogram modeling
- Calculation of ideal threshold from the modeled histogram
- Segment the subimages according to these thresholds.

At every iteration, images are split in four subimages squared of equal size (splitting them in the horizontal and vertical axes). Hereby, the process begins with an image of 512x512 pixels (in the first iteration) and can reach 256 subimages of 32x32 pixels (in the fourth iteration). For each subimage, histograms are computed and modeled as we will explain later. Different modes may be present in the histogram models and for each modeling two parameters are calculated: the number of modes and the modeling error. At every iteration, these values are compared to the ones obtained in the segmentation of the subimages of the previous iteration (that is, both values of one of the four images of any iteration are compared with the appropriate subimage of the previous iteration of which division these four subimages have appeared) If only one mode results and the modeling error is lower than the error of the subimage from previous iteration, the process finishes and the image is not split any more. However, if this mistake is higher, the division of the image continues. Independently of the number of modes of the histogram, the segmentation (previous or current iteration) that produces lowest modeling error is chosen. This modeling error is measured as the mean square error between the histogram and the histogram model, relative to the histogram itself:
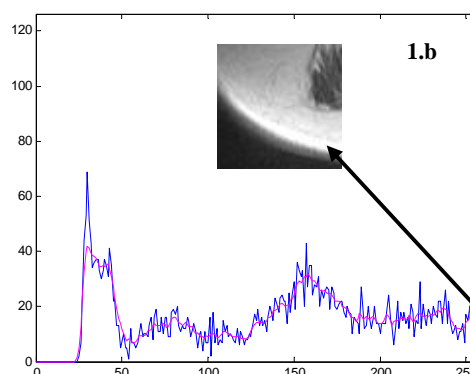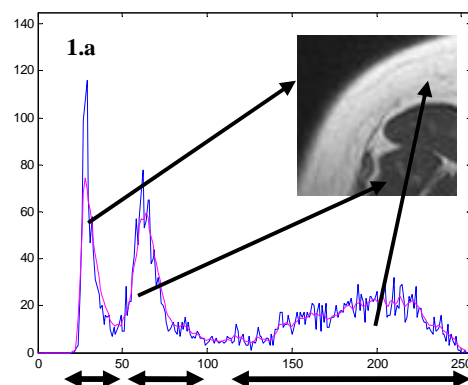
$$e_{rms} = \frac{\sum_{i=1}^{256}\left[f(z_i) - b(z_i)\right]^2}{\sum_{i=1}^{256}\left[b(z_i)\right]^2}$$

b being the histogram, f the histogram model and z the grey level, (z=1 to 256).

Every subimage is then associated to the model which has adapted best to its histogram. At every level of iterative process, the first task is to divide the input image, shape its histogram and calculate the thresholds. Histogram modeling begins with the determination of the maximum and minimum more significant peaks present in the histogram profile. The objective is to associate each maximum to a different mode.

Firstly, the modes can be represented by gaussian functions. The gradient method is used to find the parameters (weight, mean and variance) of the combination of gaussian functions that best match the histogram (Fig. 1.a).

Statistical uncertainty due to a big and imprecise number of sources (electronic noise, variability in the tissue magnetic characteristics, etc.) claims for Gaussian models for the histograms. Besides many of the computed histograms had typical bell-shaped profiles. Some other observed profiles rather resembled those of the exponential (very steep slope) or uniform (constant) functions and they are relationed to regions of intensity saturation and to noisy fragment of histogram respectively. In this situation, it is necessary to add two new modes: exponential (in the first case, Fig. 1 .b) and uniform functions (in the second case, Fig. 1 .c).

World Academy of Science, Engineering and Technology
International Journal of Biomedical and Biological Engineering
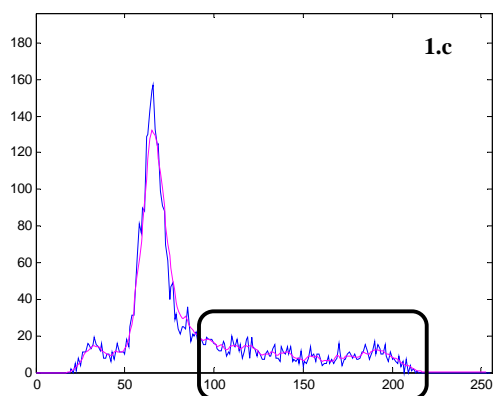Vol:3, No:10, 2009

Fig. 1: Modelling the histogram. (a) Combination of three gaussian functions, corresponding to the three main regions of the image (background, muscle and fat. (b) Image with saturated piexels, medelled with an exponential function. (c) Noise part of the histogram modeled with a uniform function.

An exponential mode is included when, due to intensity saturation, a narrow and high peak appears at the right extreme of the interval (level 255). However, to distinguish gaussian and uniform modes, subgaussianity measures are obtained from two higher order statistics: kurtosis and negentropy [10]. These statistics are calculated with the values of the pieces of the histogram obtained from the gradient method. Each mode from this method represents one fragment of the histogram, which allows to identify the set of values and to calculate kurtosis and negentropy. Modes are considered uniform when (Kur $<$-1.135 and Negen$>$1.55 E-3) or when (Kur $<$-1 and Negen$>$1.65 E-3). These values were obtained empirically. From 7 to 10 images were used to develop the method (training set). These were not removed from the evaluation set (1500 images). Being the training set such a small percentage of the whole evaluation set, overall results should not be noticeably affected by their presence.

Therefore, up to three different modes can exist in a histogram and they are represented by:

- Gaussian functions with parameters of weigth, mean and variance calculated from gradient method.
- Exponential functions of the form exp(ax+b). The coefficients will be determined by applying a log function to the measured histogram and then obtaining the a and b values by linear regression
- Uniform functions. They correspond to an interval of the histogram and are just obtained as the average value in that interval.

When the histogram is approximated by a model composed of one or several modes, thresholds are obtained to separate these modes. The threshold that separates two gaussian modes and minimize the modeling error can be obtained analytically [9]. When a pair of modes are present in the model which contain at least an exponential or a uniform mode, the threshold between them is taken at the intensity point where these two modes intersect.

Once the thresholds of each subimage are calculated, the pixels that form each connected region segmented on the image are represented graphically by the average of their intensities levels (Fig. 2).
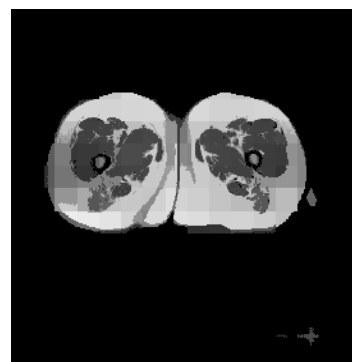

Fig. 2. Image obtained from the division and subimage segmentation stage

2) Creation of templates

Due to the division of the image, it is necessary to group the results of the segmentation of the different subimages in only three sets of pixels, corresponding to fat, muscle and rest of the image (background mainly). This second stage of the process is aimed to provide binary templates that will facilitate the grouping process, which is the last stage of the method and will be explained later (Part d of this section).

The purpose of these templates is distinguish roughly dark pixels (muscular tissue and background) from ligth pixels (adipose tissue). To increase the difference between these intensities, original image is squared. The result (image squared) is the beginning of a process which is carried out in several steps:

- *Initial segmentation*. The image squared is segmented with de lowest (darkest) threshold obtained from the histogram modeling of initial undivided image. (Fig 3.a).

- *Initial binary template*. The dark and connected pixels of the background are grouped. This result is a binary image (Fig. 3.b), which roughly distinguishes between the thighs and the background, and still has some important deficiencies as the rightmost and leftmost parts of the thigh, which have erroneously been considered as part of the background due to the effects of a poor illumination.

- *Extracting the deficient white parts*. It is necessary to include the pixels of adipose tissue affected by the poor illumination. With a more restrictive thresholding, this set of pixels can be extracted (Fig. 3.c). This new threshold is the first minimum from the histogram of the image squared (it proporciona un límite burdo entre pixels muy oscuros – background- del resto). From the image of second step (Fig.

World Academy of Science, Engineering and Technology
International Journal of Biomedical and Biological Engineering
Vol:3, No:10, 2009

3.b.) and applying connectivity operations on white pixels, the deficients white parts are obtained (Fig. 3.c.)

- Filling of the binary template. The white region of the second step (Fig 3.b) can be enlarged with the deficient white parts obtained in the previous step (Fig 3.d).

- Filling of the initial segmented image. The segmented image obtained in the first step is also filled with the deficient white parts obtained in the third step (Fig 3.e).

The results are two binary images: the first one identifies the region of the background of the image (Fig 3.d), whereas the second one will be used as guide to place the most important elements of adipose and muscular tissue (Fig.3.e).

3.e

Fig. 3. a) Initial thresholded binary image. b) Initial binary template; c) Deficiency white image d) Enlarged binary template; e) Binary image of muscle and fat distribution.

3) Bone extraction

The dark region of the bone is detected by segmenting the original image and labeling with black colour (zero intensity level) the sets of pixels with intensity levels lower than the first threshold obtained from the modeling histogram of the original image (Fig 4.a). It allows identifying the biggest connected regions within the thighs, which completely surround higher intensity pixels of the bone. The results is a binary mask to extract the bone.(Fig 4.b.)
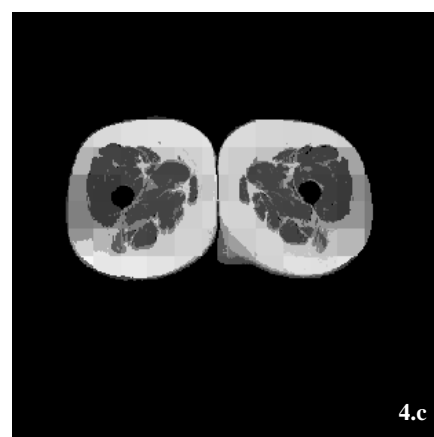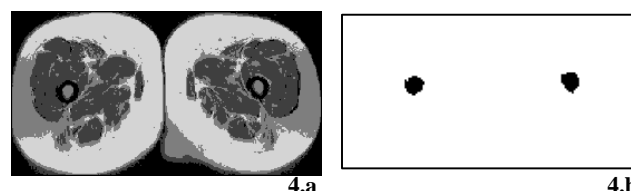
4.a

4.b

4.c

Fig. 4: Bone extraction a) Initial image after segmentation (the dark periphery of the bone appears in black) b) Bones already detected; c) Segmented image after bone extraction.

3.a

3.b

3.c

3.d

World Academy of Science, Engineering and Technology
International Journal of Biomedical and Biological Engineering
Vol:3, No:10, 2009

It is not possible to apply this technique to the images of the low part of the thigh. In this case, the information of the internal region of the bone of the previous image is used. From its contour, an iterative process of dilation operations is applied that includes new pixels up to the external border of the bone. In all the cases, a binary image (Fig. 4.b.) is obtained to extract the bone (Fig 4.c).

4) Final segmentation

At the beginning of the last stage, the image obtained from the previous steps is formed by different connected regions segmented in each subimage, with the bone extracted and with the contour of the thighs defined (Fig 4.c.).

The purpose of this step is grouping this result in an overall segmentation (Fig. 5.e). This is achieved with the information taken from three different results of the previous analyses:

-The segmentation by adaptative thresholding, resulting from the first stage of the process (Fig.5.a). It indicates the regions in which the image has been divided and the common intensity level assigned to all the pixels within that region.

- The image obtained after grouping of the different regions of Fig.2, but using the thresholds corresponding to the initial undivided image. It provides a grouping of the regions obtained in the adaptative segmentation according to the global information of the image (Fig. 5.c).

-The enlarged binary template, obtained in the last step of the stage 2) of the process (Fig. 3.e). It roughly indicates the presence of muscular (black) tissue and adipose (white) tissue in each of the regions of the segmentation (Fig.5.b).

The reason of the need to use these three results is explained here. The adaptive segmentation (AS) produces in each subimage one or several connected regions with similar intensity levels (in fact, pixels within a certain region belong to the same mode). Each of these AS regions is considered a singular part of the image, in the sense that all its pixels are represented with the same intensity level (the average of these pixels in the original image) and at the end of the processes they will be collectively assigned to the same class of tissue, either fat or muscle. The complete set of AS regions contain detail and local information about how and where different intensity levels appear in the image. This information can be very useful for the segmentation, but these regions need to be associated to muscle or fat tissue. This is the reason why other sources of information should be used for this purpose, basically:

- the image obtained after grouping of the different regions of Fig.2, using the thresholds corresponding to the initial undivided image. (Fig. 5.c),
- enlarged binary template (Fig. 3.e = Fig5.b).

The first one provides a global threshold that permits differentiating between muscle and fat and comparing the results obtained from adaptative segmentation. It is good enough when the "obscuring effect" of the sides of the thighs is not present and when the. To deal with the "obscuring effect" of the sides of the thighs and to distinguish cases when the results of adaptive and global segmentation do not agree, the enlarged binary template is used. This template has been carefully built in order to preserve the thigh contour without being affected by the "obscuring effect". Regard the white connected region in the outer part of the thigh (Fig. 3.c) that is added to Fig. 3.a to form the binary template (Fig 3.e).
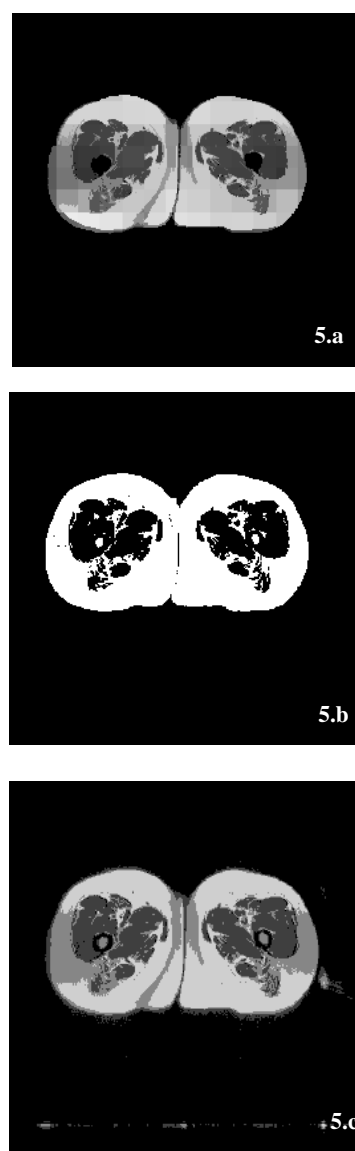

Fig. 5 (a-c): Final segmentation. a) Image segmented with adaptative thresholding and bone excluded; b) Final binary template; c) Original image segmented without applying division.

World Academy of Science, Engineering and Technology
International Journal of Biomedical and Biological Engineering
Vol:3, No:10, 2009

The process applied here (to combine the three sources of information) is an heuristic set of rules that assign for each of the regions obtained in the adaptive segmentation, one of the tissue types (fat, muscle or background). This will be decided regarding which of the histogram modes of the undivided image corresponds to the intensity level of the analysed region, and also regarding the proportion of black pixels in the enlarged binary template corresponding to that region. For instance, when an adaptative segmentation region corresponding to fat is under analysis and it suffers from the "obscuring effect", then their pixels will tend to be rather dark. In this case, the proportion of white pixels in the enlarged binary template is very high and, therefore, the region is labelled as fat tissue.
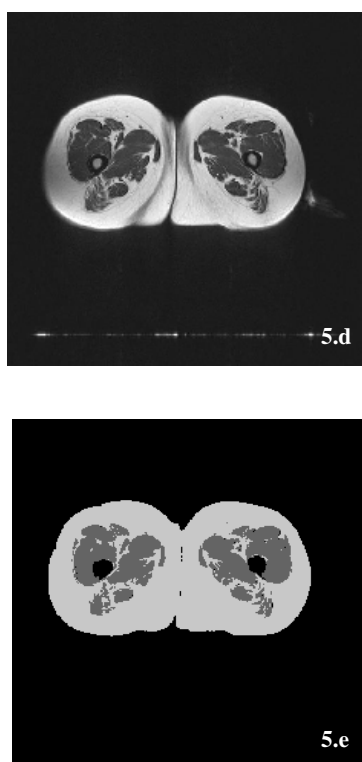

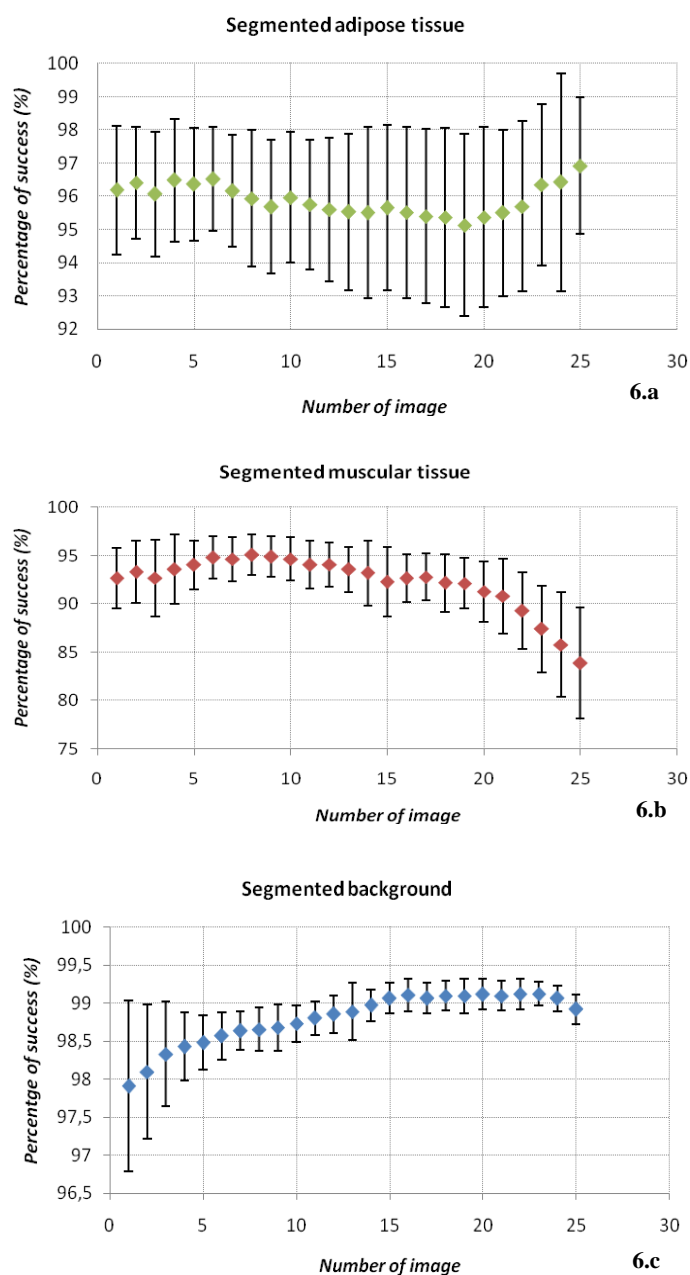Fig. 5 (d-e): Final segmentation. d) Original image; e)Final segmentation

III. RESULTS

The first 25 images (starting frorm the hip) and excluding the knee of the 30 subjects were taken for the analysis. The results of the segmentation with our method were compared to the results from the automatic approach. The number of coincidental pixels in both approaches was measured for each group (fat, muscle and rest of image). This number was normalized dividing by the number of pixels for each group obtained with the automatic approach. Mean and standard deviation of these figures are given in Fig. 6, where the abscissa axis corresponds to the number of the slice (1 being upper image, close to the hip, and 25 being the lower image, closer to the knee).

We can see that the results from the proposed method come very close to the manual technique. In the adipose tissue the rate of coincidential pixels is around 96% for all the slices. In the muscle tissue, this rate is above 90% for the first 20 slices and decreases steadily for the rest of lower slices. Finally, the background is very well detected, as the rate of coincidental pixels with the manual approach ranges from 98 to 99%.

Fig.6: Relative number of coincidental pixels in automatic and manual

approaches. (a)Adipose tissue. (b) Muscle tissue. (c) Background

World Academy of Science, Engineering and Technology
International Journal of Biomedical and Biological Engineering
Vol:3, No:10, 2009

IV. DISCUSSION

Different studies have approached the topic of the segmentation of fat and muscle of the thigh from MRIs. Although the majority of the developments are semiautomatic, recent approaches have been presented with low processing times and small external intervention [7]. Our method is fully automatic in the sense that specialist intervention is not required.

In this work, a set of 1500 images have been analysed: the first 25 images of each thigh of the 30 obese patients. The remaining 5 are near the knee. Here the intensity levels from muscular and adipose tissue are very similar and there is not a clear contrast of their edges, causing erroneous results. In addition, the presence of tendons in this area is more notorious and they cannot be segmented adequately without external intervention. This is the reason why they have been excluded from our analysis. This may also be the reason of the increase in the segmentation errors of muscle tissue in the slices 21 to 25.

Another aspect that limits the automatic processing is the darkening of the right and left parts of the images. In most cases (>96%), the enlarged binary template has managed to overcome this problem.

Finally, we have visually compared the results obtained with our method and with the manual technique, observing slightly greater detail in our results.

The average execution time of our method is about 5 minutes per image in our Matlab implementation. Obtaining the binary template is the most time consuming. This aspect could probably be improved using the similarity of consecutive slices.

V. CONCLUSION

A segmentation method that permits to separate and measure fat and mucle tissue in thigh images from MRI has been presented. The method needs no external intervention and yields results very close to those obtained by a specialist doctor following a manual procedure with the aid of the Slice-Omatic software.

REFERENCES

[1] Bonekamp, S., Gosh, P., Crawford, S., Solga, S.F., Horska, A., Brancati, F.L., Diehl, A.M., Smith, S., Clark, J.M. Quantitave comparison and evaluation of software packages for assessment of abdominal adipose tissue distribution by magnetic resonance imaging. International Journal of Obesity 32, 100-111 (2008).

[2] Goodpaster, B.H., Stenger, V.A., Boada, F., McKolanis, T., Davis, D., Ross, R., Kelley, D. E. Skeletal muscle lipid concentration quantified by magnetic resonance imaging. Am J Clin Nutr 79,748-54 (2004)

[3] Gronemeyer, S.A., Grant, R., Kauffman, W.M., Reddick, W.E, Glass, J.O. Fast adipose tissue (FAT) assessment by MRI. Magnetic Resonance Imaging 18,815-818 (2000)

[4] Poll, L.W, Wittsack, H.J., Koch, J.A, Willers, R., Cohnen, M., Kapitza, C., Heinemann, L., Mödder, U. A rapid and reliable semiautomated method for measurement of total abdominal fat volumes using magnetic resonance imaging. Magnetic Resonance Imaging 21, 631-636 (2003)

[5] Barra, V., Boire, J.Y. Segmentation of fat and muscle from MR images of the thigh by a possibilistis clustering algorithm. Computer Methods and Programs in Biomedicine 68, 185-193 (2002)

[6] Positano, V., Gastaldelli, A., Sironi, A.M., Santarelli, M.F., Lombardi, M., Landini, L. An accurate and robust method for unsupervised assessment of abdominal fat by MRI. Journal of MRI 20:684-689 (2004)

[7] Positano, V., Christiansen, T., Santarelli, M.F., Ringaard, S., Landini, L., Gastaldelli, A. Accurate segmentation of subcutaneous and intermuscular adipose tissue from MR images of the thigh. Journal of MRI 29, 677-684 (2009)

[8] Liou, T.H., Chan, W.P., Pan, L.C., Lin, P.W., Chou, P., Chen, C.H. Fully automated largescale assessment of visceral and subcutaneous abdominal adipose tissue by magnetic resonance imaging. International Journal of Obesity 30, 844–852 (2006).

[9] Gonzalez, R. C., Woods, R.E. Digital Signal Processing (2nd ed.). Prentice-Hall, 2001.

[10] Hivarinen, A., Kahunen, J., Oja, E., Independent Component Analysis, John Wiley & Sons, 2001.